Title

Chemoproteomic Approach toward Probing the Interactomes of Perfluoroalkyl Substances

Journal

Analytical Chemistry, 93(27)

ISSN

0003-2700

Authors

Zhang, Quanqing
Dong, Xuejiao
Lu, Jiuwei
et al.

Publication Date

2021-07-13

DOI

10.1021/acs.analchem.1c01948

Peer reviewed

HHS Public Access

Author manuscript

Anal Chem. Author manuscript; available in PMC 2022 July 13.

Published in final edited form as:

Anal Chem. 2021 July 13; 93(27): 9634–9639. doi:10.1021/acs.analchem.1c01948.

Chemoproteomic Approach toward Probing the Interactomes of Perfluoroalkyl Substances

Quanqing Zhang,
Department of Chemistry, University of California, Riverside, California 92521, United States

Xuejiao Dong,
Department of Chemistry, University of California, Riverside, California 92521, United States

Jiuwei Lu,
Department of Biochemistry, University of California, Riverside, California 92521, United States

Jikui Song,
Department of Biochemistry, University of California, Riverside, California 92521, United States

Yinsheng Wang
Department of Chemistry, University of California, Riverside, California 92521, United States

Abstract

Poly- and perfluoroalkyl substances (PFASs) are widely used in industrial products and consumer goods. Due to their extremely recalcitrant nature and potential bioaccumulation and toxicity, exposure to PFASs may result in adverse health outcomes in humans and wildlife. In this study, we developed a chemoproteomic strategy, based on the use of isotope-coded desthiobiotin-perfluorooctanephosphonic acid (PFOPA) probe and liquid chromatography with tandem mass spectrometry (LC-MS/MS) analysis, to profile PFAS-binding proteins. Targeted proteins were labeled with the desthiobiotin-PFOPA probe, digested with trypsin, and the ensuing desthiobiotin-conjugated peptides were enriched with streptavidin beads for LC-MS/MS analysis. We were able to identify 469 putative PFOPA-binding proteins. By conducting competitive binding experiments using low (10 μM) and high (100 μM) concentrations of stable isotope-labeled PFOPA probes, we further identified 128 nonredundant peptides derived from 75 unique proteins that exhibit selective binding toward PFOPA. Additionally, we demonstrated that one of these proteins, fatty acid-binding protein 5 (FABP5), could interact directly with PFASs, including perfluorooctanoic acid (PFOA), perfluorooctanesulfonic acid (PFOS), perfluorohexanesulfonic acid (PFHxS), and perfluorobutanesulfonic acid (PFBS). Furthermore, desthiobiotin-labeled lysine residues are

Corresponding Author: Yinsheng Wang – Department of Chemistry, University of California, Riverside, California 92521, United States; Phone: (951)827-2700; Yinsheng.Wang@ucr.edu.

Supporting Information

The Supporting Information is available free of charge at https://pubs.acs.org/doi/10.1021/acs.analchem.1c01948.

Synthetic scheme, ESI-MS and MS/MS of the synthetic desthiobiotin-PFOPA acyl phosphate probes, and representative MS/MS of desthiobiotin-modified peptides of select PFOPA-binding proteins (PDF)

Excel tables summarizing the quantification results; FPLC trace and SDS-PAGE for monitoring the purification of FABP5 protein, and ITC traces for monitoring the binding affinities between FABP5 and PFASs; all proteomics data have been deposited to the ProteomeXchange Consortium via the PRIDE partner repository39 with the data set identifier: PXD025757 (XLSX)

Complete contact information is available at: https://pubs.acs.org/10.1021/acs.analchem.1c01948

The authors declare no competing financial interest.

located close to the fatty acid-binding pocket of FABP5, and the binding affinity varies with the structures of PFASs. Taken together, we developed a novel chemoproteomic method for interrogating the PFAS-interacting proteome. The identification of these proteins sets the stage for understanding the mechanisms through which exposure to PFASs confers adverse human health effects.

Graphical Abstract

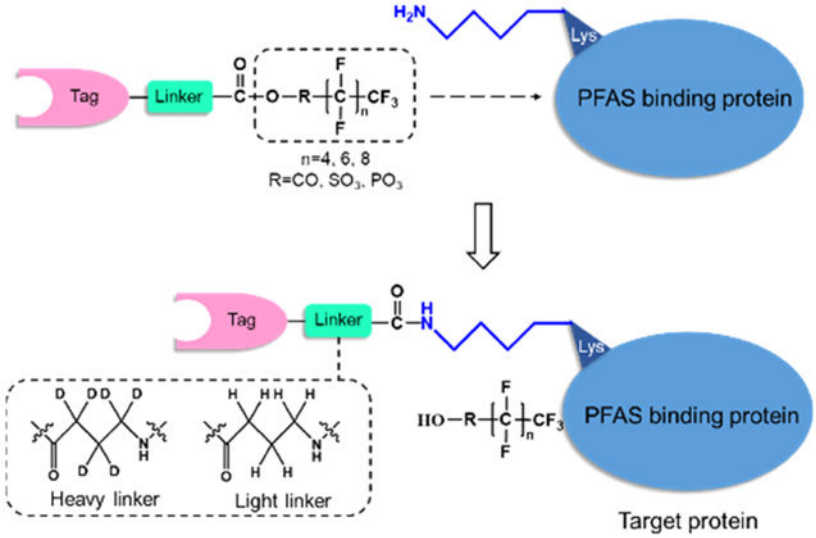

Poly- and perfluoroalkyl substances (PFASs) are compounds with fluorocarbon chains and a variable ionic or neutral functional group.[1] Various PFASs, especially perfluorooctanoic acid (PFOA) and perfluorooctanesulfonic acid (PFOS), are widely used chemicals,[2–4] where approximately 4000 different PFASs have been used in industrial and consumer products.[1,5] Owing to their environmental persistence, toxicity, and resistance to conventional treatment processes, PFAS contaminations are widespread.[6,7] In the past few decades, short-chain PFASs, e.g., perfluoroalkyl carboxylic acid and perfluoroalkyl sulfonic acid with fewer than six carbon atoms, were thought to be less toxic and became widely used.[8,9] Several recent studies, however, showed that these short-chain PFASs are more persistent and have toxicity concerns on their own.[10–15] The current remediation strategy for PFASs in contaminated water was through affinity adsorption with activated carbons.[16] Nevertheless, the activated carbons' limited affinity for short-chain PFASs renders their removal processes inefficient.[15]

Some initial studies have been conducted for identifying PFAS-binding proteins. It was found that PFASs (PFOS and PFOA) exhibit strong binding with fatty acid-binding protein 1 (FABP1), which may contribute to augmented liver weight in exposed animals.[1,17–19] In addition, Shao et al.[20] reported the use of two cysteine-reactive probes, iodoacetamide alkyne and ethynyl benziodoxolone azide, to enrich putative target proteins in the absence or presence of PFOA, and quantitative proteomic analysis of the resulting enriched proteins led to the identification of Acaca and Acacb as interaction proteins of PFOA. When applied for complex samples, these strategies, however, display limited abilities in identifying specific PFAS-binding proteins of low abundance. Therefore, there is a need of analytical

methods for the systematic discovery of PFAS-interacting proteins and for understanding the implications of these interactions in the toxic mechanisms of action of PFASs.

In recent years, activity-based protein profiling was developed to identify candidate target proteins with the use of chemical probes that can bind to and react with specific amino acid residues near the ligand-binding sites of proteins.[21] Moreover, this strategy could allow for efficient removal of contaminated proteins through on-bead enrichment, thereby enabling facile identification of ligand-binding proteins.[22,23] Previously, our laboratory developed several chemical probes, which, in conjunction with liquid chromatography with tandem mass spectrometry (LC-MS/MS) analysis, led to the proteome-wide discoveries of interaction proteins of lysophosphatic acid,[24] isoprenoids,[25] and adenosine 5′-triphosphate/guanosine 5′-triphosphate (ATP/GTP).[26,27]

Herein, we established a chemoproteomic strategy for the identification, at the proteome-wide level, of PFAS-binding proteins, and the method capitalizes on the use of isotope-labeled desthiobiotin-perfluorooctanephosphonic acid probe and LC-MS/MS analysis. We also demonstrated that one of the newly identified proteins, FABP5, could bind directly with PFASs.

EXPERIMENTAL SECTION

Materials.

Chemicals, unless otherwise specified, were from Sigma-Aldrich (St. Louis, MO) or Thermo Fisher Scientific (Pittsburg, PA).

Syntheses and Purification of Desthiobiotin-PFOPA Affinity Probes.

All air and/or moisture-sensitive reactions were performed under an argon atmosphere using flame/oven-dried glassware and standard septa/syringe techniques.

The probes were synthesized in two steps, where we first prepared light and heavy stable isotope-labeled desthiobiotinyl-γ-aminobutyric acid (desthiobiotin-C4) following previously published procedures with minor modifications.[28] In brief (Scheme S1), to a stirring 2 mL solution of desthiobiotin (170 mg) and *N*-hydroxysuccinimide (101 mg) in dimethylformamide (DMF) under an argon atmosphere, was added *N*,*N*′-dicyclohexylcarbodiimide (DCC, 181.2 mg in 2 mL of DMF). The solution was stirred at room temperature for 10 h. The reaction mixture was filtered, and the filtrate was collected and dried to yield desthiobiotin-NHS. Desthiobiotin-NHS (62.4 mg) and γ-aminobutyric acid or [D_6]-γ-aminobutyric acid (44 mg) were added to tri-*n*-butylamine (190 μL), and the solution was stirred for 16 h. The desired desthiobiotin-C4 was precipitated out of the solution. The product was purified with silica-gel column chromatography using CH_2Cl_2/CH_3OH (5:1, v/v) as the mobile phase. The precipitate was then washed with water and dried under vacuum.

Isobutyl chloroformate (7.8 μL) was dropwise added to a 0.4 mL of ice-cooled DMF solution containing desthiobiotin-C4 (18 mg), tri-*n*-butylamine (28.6 μL), and 1.2 mL of CH_2Cl_2. After stirring for 30 min, the solution was raised to room temperature and stirred

for another 1.5 h under an argon atmosphere. PFOPA (8 mg), dissolved in 0.5 mL solution of CH_2Cl_2 and DMF (4:1, v/v), was subsequently added, and the reaction was continued for another 16 h. The prepared desthiobiotin-PFOPA affinity probes were purified using flash column chromatography with a silica-gel column and a step gradient, where the mobile phases included 5% CH_3OH in CH_2Cl_2 (100 mL), 6.67% CH_3OH in CH_2Cl_2 (100 mL), and 10% CH_3OH in CH_2Cl_2 (300 mL). The desired fractions were pooled and dried by rotary evaporation. The structures of the prepared desthiobiotin-PFOPA probes were confirmed by electrospray ionization-MS (ESI-MS) analysis.

Cell Culture, Lysate Preparation, and Labeling with the PFOPA Probe.

Cells were maintained at 37 °C in a humidified incubator with 5% CO_2 and cultured in Dulbecco's modified Eagle's medium (DMEM) supplemented with 10% fetal bovine serum (FBS), 100 U/mL penicillin, and 100 μg/mL streptomycin. The cells were subsequently harvested by centrifugation, and the ensuing cell pellets were washed with ice-cold phosphate-buffered saline (PBS) and stored at −80 °C until use.

To prepare whole-cell lysates, the frozen cell pellet was resuspended in a hypotonic buffer, which contained 10 mM 4-(2-hydroxyethyl)-1-piperazineethanesulfonic acid (HEPES) (pH 7.5), 2 mM $MgCl_2$, 0.1% Tween-20, 20% glycerol, 2 mM phenylmethylsulfonyl fluoride (PMSF), and Complete ethylenediaminetetraacetic acid (EDTA)-free protease inhibitors (Roche). After incubation at 4 °C for 10 min, the suspension was centrifuged at 16 000*g* for 15 min at 4 °C. The resulting cell pellet was collected and reconstituted in a high-salt buffer (50 mM HEPES, pH 7.5, 420 mM NaCl, 2 mM $MgCl_2$, 0.1% Tween-20, 20% glycerol, 2 mM PMSF, and complete EDTA-free protease inhibitors) and incubated at 4 °C for 30 min. The suspension was centrifuged at 16 000*g* for 15 min at 4 °C, and the supernatant was combined with the soluble fraction in the above-described hypotonic buffer to give the whole-cell protein lysate. The protein concentration of the whole-cell lysate was quantified using Bradford assay.

The above-prepared whole-cell lysate was diluted to a final concentration of 1 mg/mL, and to 0.5 mg of the lysate were added $MgCl_2$, $CaCl_2$, and $CuCl_2$ until their final concentrations were 50, 5, and 0.5 mM, respectively. The desthiobiotin-PFOPA probe (Table S1) was subsequently added to the mixture, and the solution was incubated at 4 °C for 2 h. The resulting proteins were then dissolved in a 1 mL solution of 8 M urea, reduced with dithiothreitol (20 mM) at 37 °C for 60 min, and alkylated with iodoacetamide (55 mM) at room temperature in the dark for 0.5 h. The solution was buffer exchanged to 50 mM ammonium bicarbonate using a 10 kDa molecular weight cut-off filter. The solution was then incubated with trypsin at an enzyme/substrate ratio of 1:50 (w/w) at 37 °C overnight. The desthiobiotin-labeled peptides were enriched from the ensuing mixture using high-capacity streptavidin agarose beads (Thermo Fisher Scientific), where the suspension was mixed using a rotating shaker at 4 °C for 2 h. The pooled samples were washed sequentially with 10× PBS, 1× PBS, and water for three times each. The peptides were eluted with a 300 μL of buffer containing 0.1% trifluoroacetic acid (TFA) in CH_3CN/H_2O (7:3, v/v) at room temperature. The solution was dried using a Speed-vac and desalted using

C18 zip-tips (Waters). The peptide solution was then dried by Speed-vac and stored at −80 °C until LC-MS/MS analysis.

LC-MS/MS Analysis and Database Search.

The peptide samples were dissolved in a 20 μL solution of 0.1% formic acid and injected for LC-MS/MS analysis on a Q Exactive Plus quadrupole-Orbitrap mass spectrometer (Thermo Fisher Scientific). First, the peptide samples were loaded onto a precolumn (75 μm in internal diameter and 4 cm in length) packed in house with reversed-phase C18 material (ODS-AQ C18, 5 μm in particle size, Dr. Maisch GmbH HPLC). The analytes were subsequently resolved on an analytical column (75 μm I.D., 25 cm in length) packed with reversed-phase C18 material (ReproSil-Pur 120 C18-AQ, 3 μm in particle size, Dr. Maisch GmbH HPLC). The mobile phases were 0.1% formic acid in water (buffer A) and 0.1% formic acid in CH_3CN (buffer B). The gradient included 0–15 min, 95% A; 15–150 min, 95–63% A; 150–152 min, 63–1% A; 152–179 min, 1% A; 179–179.01 min, 1–95% A; and 179.01–200 min, 95% A. The flow rate was 300 nL/min.

The mass spectrometer was operated in a data-dependent acquisition mode, where one full-scan MS (m/z 300–2000) was followed by MS/MS scans on the 20 most abundant ions found in full-scan MS. Precursor ions were isolated at a width of 1.0 m/z unit, and dynamic exclusion was enabled with an exclusion time window of 60 s after a precursor ion was first selected for MS/MS acquisition. The raw data were processed and analyzed using MaxQuant (version 1.5.2.8). A human fasta file (ipi.HUMAN.v.3.68.fasta) was employed as the database for protein identification with the use of default parameters. Lysine C4-desthiobiotinylation (light: $C_{14}H_{23}O_3N_3$, +281.1739; heavy: $C_{14}H_{17}D_6O_3N_3$, +287.2116) and methionine oxidation were considered as variable modifications. Cysteine carbamidomethylation was set as a fixed modification. The reverse database search option was enabled to filter the search results to satisfy a maximum false discovery rate of 1%. In addition, mass tolerances for precursor and fragment ions were 6 and 10 ppm, respectively, the minimum peptide length was six amino acids, and the maximum number of missed cleavages for trypsin was 2. The proteins quantified were supported by at least two quantification replicates.

Purification of Recombinant Fatty Acid-Binding Protein 5 (FABP5).

The plasmid for the expression of recombinant His_6-tagged human FABP5 was purchased from DNASU at Arizona State University. The construct was transfected into BL21 *Escherichia coli* cells. The bacteria were cultured, at 37 °C with shaking, in Luria broth (LB) medium containing 50 μg/mL of kanamycin until OD600 of the culture reached 0.6–0.8. IPTG was subsequently added until its final concentration was 1.0 mM, and the culture was grown at 16 °C for an additional 16 h. The cells were harvested by centrifugation at 5000 rpm at 4 °C, resuspended in 10 mM Tris–HCl (pH 7.2), and lysed by sonication on ice. The supernatant was collected after centrifugation. The crude cell extract, containing the desired His-tagged proteins, was loaded onto a HisTrap HP column (GE Healthcare) and washed with a buffer containing 5 mM imidazole. The desired protein was eluted with a buffer containing 300 mM imidazole. The ensuing FABP5 protein was subsequently delipidated by passing through a home-made hydroxyalkoxypropyl dextran (Type VI) column and finally

purified with size-exclusion chromatography on a Superdex 200 Increase 10/300 column (GE Healthcare), where the protein was eluted with PBS buffer at a flow rate of 0.75 mL/min. The resulting protein solution was dialyzed against a storage buffer containing 50 mM Tris (pH 7.5), 30 mM NaCl, and 5% glycerol. The purity of the His-tagged protein was verified by sodium dodecyl sulfate-polyacrylamide gel electrophoresis (SDS-PAGE) analysis.

Isothermal Titration Calorimetry (ITC) Analysis.

The ITC experiments for FABP5 were performed on a MicroCal iTC200 isothermal titration calorimeter (Malvern, U.K.). In particular, the FABP5 solution was placed in the sample cell. The reference cell with water and the sample cell with 0.1 mM FABP5 were set at 25 °C. PFAS solution (1 mM) was loaded into a syringe. In titration experiments, both the FABP5 and PFAS were dissolved in a buffer containing 100 mM NaCl, 30 mM Tris (pH 7.5), and 5% glycerol. A series of small aliquots of ligand were injected into the protein solution with a 180 s time interval between neighboring injections, beginning with an initial 0.5 μL injection and followed by 16 × 2.43 μL injections. The solution was stirred at 1000 rpm throughout the experiment, and heat changes were measured. After the titration, the data were analyzed using MicroCal ITC-Origin analysis software and fit with the one-binding-site model to determine the dissociation constant and the error of the fit.

RESULTS AND DISCUSSION

Design of PFOPA Probes.

In this study, we set out to design a chemical probe for the proteome-wide identification of PFAS-binding proteins. On the grounds that biotin- or desthiobiotin-conjugated acyl phosphate probes were previously employed for proteome-wide discovery of those proteins that can bind to phosphate-containing small molecules,[29–31] we designed a desthiobiotin-PFOPA acyl phosphate probe for profiling PFOPA-binding proteins.

As illustrated in Figure 1, the binding of the desthiobiotin-PFOPA probe to cellular proteins promotes the nucleophilic reaction between the carbonyl carbon of acyl phosphate and the side-chain amino group of lysine residue(s) located near or at the binding site, thereby installing a desthiobiotin to PFOPA-interaction proteins and enabling subsequent affinity enrichment using streptavidin resin. Owing to the nature of the probe design, the identification of probe-labeled lysine could also assist the localization of PFAS-binding site(s) in proteins. In this vein, we incorporated a γ-aminobutyryl (GABA) linker between PFOPA and the desthiobiotin affinity tag to minimize the influence of desthiobiotin tag on PFOPA–protein interactions. Moreover, the GABA linker can be introduced in light- or heavy-labeled form (i.e., with six hydrogen or deuterium atoms), which enables quantitative proteomic analysis (Figure 1). We synthesized the probes and confirmed their identities by ESI-MS and MS/MS (Figure S1).

Shotgun Proteomics for Profiling PFOPA-Binding Proteins.

We next employed a shotgun proteomic method to identify candidate PFOPA-binding proteins. To this end, we first treated the whole-cell protein lysate with the light

desthiobiotin-PFOPA probe, digested the protein mixture with trypsin, enriched the resulting desthiobiotin-labeled peptides with streptavidin beads, and analyzed the sample using LC-MS/MS. Analysis of the LC-MS/MS data showed that, with 1 mg of protein lysate in a 1 mL of solution, the use of 10 and 100 μM probe led to the identifications of 653 and 1286 proteins (Figure S2).

A previous study showed that FABP1 can bind to PFOA, which may contribute to the accumulation of PFASs in the liver and the development of liver steatosis.[32] Here, our shotgun proteomic data led to the identification of FABP5, another member of the FABP family, as one of candidate PFAS-binding proteins. FABP5 is a lipid- and fatty acid-binding protein.[33] It is of note that our proteomic data did not lead to the identification of FABP1 as a PFOPA-binding protein, which is very likely attributed to the low level of expression of this protein in HEK293T cells. Along this line, it was shown that FABP1 was not detectable at the mRNA or protein level in HEK293 cells.[34,35]

Based on the structural similarity between PFASs and fatty acids, we reason that PFASs may occupy the fatty acid-binding pocket of the protein. As depicted in Figure 2, helix 1, helix 2, and loop 1 constitute the portal domain, which is the ligand access gate of FABPs.[36] When a 100 μM probe was employed for the labeling experiment, all of the three identified peptides of FABP5 were located near this domain. For the three lysine residues labeled with the probe, K34 and K55 face outward the pocket, whereas K61 faces inward the pocket. In this regard, it is worth noting that, other than the mass shifts in y and b ions containing the modified lysine residue, we also observed a characteristic fragment ion arising from the desthiobiotin-GABA remnant (m/z 282.19) in the MS/MS for the modified lysine-containing peptides (representative MS/MS are shown in Figure S3). Hence, this fragment ion may be employed for confirming the presence of desthiobiotin modification in peptides.

We also found that the MS signal intensity for the K61-containing peptide is approximately 10-fold higher than those of K34- and K55-bearing tryptic peptides. In addition, only K61, but not K34 or K55, was labeled when a low concentration of probe (10 μM) was employed. The electrostatic potential map for FABP5 revealed an obvious binding channel at or near the binding site, where the labeled K61 is situated at the entrance of the binding pocket (Figure 2). This result, therefore, supports that the PFOPA binds to the fatty acid-binding pocket of FABP5.

Stable Isotope-Labeled Probes for Profiling PFOPA-Binding Proteins.

The inherent chemical reactivity of acyl phosphate may also lead to nonspecific labeling of cellular proteins with desthiobiotin. To identify specific PFAS-binding proteins, we conducted a competitive labeling experiment with a high (100 μM) concentration of light-labeled probe and a low (10 μM) concentration of the heavy-labeled PFOPA probe (Figure 3). In this vein, a similar competitive labeling strategy was previously employed for identifying reactive cysteine-containing proteins, as well as lysophosphatic acid-, GTP-, and isoprenoid-binding proteins.[22,24,25,27] The principle behind this experiment is that, with a low concentration of the probe (10 μM), labeling occurs preferentially for those proteins with specific binding to the probe, whereas both specific and nonspecific PFOPA-binding proteins are labeled with a high concentration of the probe (100 μM). It is worth noting a

potential limitation of this competitive labeling method. In particular, labeling efficiencies for some low-abundance proteins may be similar with 10 and 100 μM of probe; as a result, this may give rise to false-positive identification of PFOPA-binding proteins.

We first confirmed that the concentrations of the stock solutions of the light- and heavy-labeled probes were the same by ESI-MS analysis (Figure S4). The experiment led to the identification of 128 unique peptides representing 75 distinct proteins with heavy/light ratio being less than 3.0 (Table S1). All of the 128 peptides were identified from at least one forward and one reverse labeling experiments. FABP5 is still among these 75 proteins and has an average ratio of 1.64, suggesting the specific binding of FABP5 with PFOPA.

Gene ontology (GO) analysis of the protein list showed several highly enriched GO terms, where metabolic processes were highly enriched in the biological process clustering (Figure S5). Based on molecular function analysis, we found that, aside from FABP5, nine other lipid-binding proteins were identified (Figure S6), perhaps due to the structural similarity between PFASs and lipids. Moreover, on the basis of disease ontology semantic and enrichment analysis, we found that several identified proteins are highly associated with human diseases, including Alzheimer's disease (Figures S7 and S8).

FABP5 Binds Directly with PFASs.

The aforementioned proteomic data led to the identification of FABP5 as a candidate PFAS-binding protein. We next examined whether the protein can bind directly with PFASs. To this end, we first purified recombinant His-tagged FABP5 protein using affinity chromatography, delipidated the protein using a hydroxyalkoxypropyl dextran (Type VI) column, and further purified the protein using fast protein liquid chromatography (FPLC). We next employed isothermal titration calorimetry (ITC) to measure the binding affinities between recombinant FABP5 (Figure S9) and PFASs. As shown in Figures 4 and S10, the ITC results revealed the direct interaction between FABP5 and PFOPA with a dissociation constant (K_d) of 167 ± 34 μM. Given that PFOA is a well-known binding target of FABP1,[14,17] we also measured the binding affinity between FABP5 and PFOA, which yield a K_d value of 77 ± 17 μM.

Recent studies showed that bioaccumulation of PFASs is positively correlated with the length of their alkyl chains.[37] Hence, we also assessed the binding affinities of the protein toward three commercially available perfluorosulfonic acid derivatives with different alkyl chain length, i.e., PFOS, perfluorohexanesulfonic acid (PFHxS), and perfluorobutanesulfonic acid (PFBS), and the K_d values were 135 ± 7, 188 ± 39, and 66 ± 13 μM, respectively. Thus, the binding affinities of PFASs toward FABP5 increase with the length of the alkyl chain. This finding, which parallels with the previous observations for FABP1.[38,39]

CONCLUSIONS

In summary, we synthesized stable isotope-labeled desthiobiotin-PFOPA affinity probes and demonstrated that the use of these probes, in combination with LC-MS/MS analysis, allowed for the facile identification and quantification of PFAS-binding proteins. We were

able to identify 469 candidate PFOPA-binding proteins. We further employed a competition labeling experiment with the use of a low and a high concentration of isotopically labeled desthiobiotin-PFOPA probes to discover protein targets that can bind specifically to PFOPA. The experiment led to the identification of 128 peptides originating from 75 unique proteins that can bind specifically to PFOPA. GO analysis indicates that most of the possible binding targets are associated with metabolic processes and related diseases. The method also allows for the discovery of lysine residue(s) located at and/or near PFAS-binding sites, which afforded important information about the potential binding sites in target proteins. Nevertheless, a limitation of the probe resides in that it does not allow for the identification of PFAS-binding proteins which do not carry a lysine residue at or near the ligand-binding site.

We also demonstrated that, among the candidate proteins, FABP5 can bind directly with PFASs, where binding affinities are affected by the chemical structures of the PFASs. Based on the previously reported crystal structure of the protein, we also found that the desthiobiotin-labeled lysine residues are located in the entrance portal of the fatty acid-binding pocket of FABP5.

Taken together, our approach, involving the use of stable isotope-labeled desthiobiotin-PFOPA probes and LC-MS/MS analysis, constitutes a powerful method for the identification and quantification of PFAS-binding proteins. In addition, the method obviates the needs of metabolic labeling of the proteome, and it can be envisaged that the method can be amenable for tissue samples that are not readily subjected to stable isotope labeling by amino acids in cell culture (SILAC) labeling.

Supplementary Material

Refer to Web version on PubMed Central for supplementary material.

ACKNOWLEDGMENTS

The authors would like to thank the National Institutes of Health for supporting this work (R35 ES031707 to Y.W. and R35 GM 119721 to J.S.).

REFERENCES

(1). Cheng W; Ng CA Environ. Sci. Technol 2018, 52, 7972–7980. [PubMed: 29897239]
(2). Van den Bergh M; Krajnc A; Voorspoels S; Tavares SR; Mullens S; Beurroies I; Maurin G; Mali G; De Vos DE Angew. Chem., Int. Ed 2020, 59, 14086–14090.
(3). Klemes MJ; Ling Y; Ching C; Wu C; Xiao L; Helbling DE; Dichtel WR Angew. Chem., Int. Ed 2019, 58, 12049–12053.
(4). Greenhill C Nat. Rev. Endocrinol 2017, 13, No. 377.
(5). Wang Z; DeWitt JC; Higgins CP; Cousins IT Environ. Sci. Technol 2017, 51, 2508–2518. [PubMed: 28224793]
(6). Beach SA; Newsted JL; Coady K; Giesy JP Rev. Environ. Contam. Toxicol 2006, 186 186, 133–174. [PubMed: 16676904]
(7). Rao U; Su Y; Khor CM; Jung B; Ma S; Cwiertny DM; Wong BM; Jassby D Environ. Sci. Technol 2020, 54, 10668–10677. [PubMed: 32786552]

(8). Nian M; Luo K; Luo F; Aimuzi R; Huo X; Chen Q; Tian Y; Zhang J Environ. Sci. Technol 2020, 54, 8291–8299. [PubMed: 32525661]

(9). Conder JM; Hoke RA; De Wolf W; Russell MH; Buck RC Environ. Sci. Technol 2008, 42, 995–1003. [PubMed: 18351063]

(10). Wang Z; Cousins IT; Scheringer M; Hungerbuehler K Environ. Int 2015, 75, 172–179. [PubMed: 25461427]

(11). Wang Z; Cousins IT; Scheringer M; Hungerbuhler K Environ. Int 2013, 60, 242–248. [PubMed: 24660230]

(12). Yang AN; Ching CS; Easier M; Helbling DE; Dichtel WR ACS Mater. Lett 2020, 2, 1240–1245.

(13). Gomis MI; Vestergren R; Borg D; Cousins IT Environ. Int 2018, 113, 1–9. [PubMed: 29421396]

(14). Sheng N; Cui R; Wang J; Guo Y; Wang J; Dai J Arch. Toxicol 2018, 92, 359–369. [PubMed: 28864880]

(15). Sun M; Arevalo E; Strynar M; Lindstrom A; Richardson M; Kearns B; Pickett A; Smith C; Knappe DRU Environ. Sci. Technol. Lett 2016, 3, 415–419.

(16). Eschauzier C; Beerendonk E; Scholte-Veenendaal P; De Voogt P Environ. Sci. Technol 2012, 46, 1708–1715. [PubMed: 22201258]

(17). Sheng N; Li J; Liu H; Zhang A; Dai J Arch. Toxicol 2016, 90, 217–227. [PubMed: 25370009]

(18). Cao HM; Zhou Z; Wang L; Liu GL; Sun YZ; Wang YW; Wang T; Liang Y Environ. Sci. Technol 2019, 53, 2811–2819. [PubMed: 30735364]

(19). Yang C; Lee HK; Zhang Y; Jiang LL; Chen ZF; Chung ACK; Cai Z Anal. Chem 2019, 91, 8783–8788. [PubMed: 31251037]

(20). Shao X; Ji F; Wang Y; Zhu L; Zhang Z; Du X; Chung ACK; Hong Y; Zhao Q; Cai Z Anal. Chem 2018, 90, 11092–11098. [PubMed: 30134650]

(21). Lanning BR; Whitby LR; Dix MM; Douhan J; Gilbert AM; Hett EC; Johnson TO; Joslyn C; Kath JC; Niessen S; Roberts LR; Schnute ME; Wang C; Hulce JJ; Wei B; Whiteley LO; Hayward MM; Cravatt BF Nat. Chem. Biol 2014, 10, 760–767. [PubMed: 25038787]

(22). Weerapana E; Wang C; Simon GM; Richter F; Khare S; Dillon MB; Bachovchin DA; Mowen K; Baker D; Cravatt BF Nature 2010, 468, 790–795. [PubMed: 21085121]

(23). Hacker SM; Backus KM; Lazear MR; Forli S; Correia BE; Cravatt BF Nat. Chem 2017, 9, 1181–1190. [PubMed: 29168484]

(24). Dong X; Gao L; Song J; Wang Y Anal. Chem 2019, 91, 15365–15369. [PubMed: 31765128]

(25). Cai R; Huang M; Wang Y Anal. Chem 2018, 90, 14339–14346. [PubMed: 30433760]

(26). Miao W; Li L; Wang Y Anal. Chem 2018, 90, 6835–6842. [PubMed: 29722524]

(27). Xiao Y; Ji D; Guo L; Wang Y Anal. Chem 2014, 86, 4550–4558. [PubMed: 24689502]

(28). Qiu HB; Wang YS Anal. Chem 2007, 79, 5547–5556. [PubMed: 17602667]

(29). Guo L; Xiao Y; Wang Y Anal. Chem 2014, 86, 10700–10707. [PubMed: 25301106]

(30). Huang Q; Zhang J; Peng S; Du M; Ow S; Pu H; Pan C; Shen HJ Appl. Toxicol 2014, 34, 1342–1351.

(31). Miao W; Xiao Y; Guo L; Jiang X; Huang M; Wang Y Anal. Chem 2016, 88, 9773–9779. [PubMed: 27626823]

(32). Cao H; Zhou Z; Wang L; Liu G; Sun Y; Wang Y; Wang T; Liang Y Environ. Sci. Technol 2019, 53, 2811–2819. [PubMed: 30735364]

(33). Field CS; Baixauli F; Kyle RL; Puleston DJ; Cameron AM; Sanin DE; Hippen KL; Loschi M; Thangavelu G; Corrado M; Edwards-Hicks J; Grzes KM; Pearce EJ; Blazar BR; Pearce EL Cell. Metab 2020, 31, 422–437 e425. [PubMed: 31883840]

(34). Geiger T; Wehner A; Schaab C; Cox J; Mann M Mol. Cell. Proteomics 2012, 11, No. M111.014050.

(35). Thul PJ; Åkesson L; Wiking M; Mahdessian D; Geladaki A; Blal HA; Alm T; Asplund A; Björk L; Breckels LM; Bäckström A; et al. Science 2017, 356, No. eaal3321. [PubMed: 28495876]

(36). Armstrong EH; Goswami D; Griffin PR; Noy N; Ortlund EA J. Biol. Chem 2014, 289, 14941–14954. [PubMed: 24692551]

(37). Xu Y; Fletcher T; Pineda D; Lindh CH; Nilsson C; Glynn A; Vogs C; Norstrom K; Lilja K; Jakobsson K; Li Y Environ. Health Perspect 2020, 128, No. 077004.

(38). Zhang L; Ren XM; Guo LH Environ. Sci. Technol 2013, 47, 11293–11301. [PubMed: 24006842]

(39). Perez-Riverol Y; Csordas A; Bai J; Bernal-Llinares M; Hewapathirana S; Kundu DJ; Inuganti A; Griss J; Mayer G; Eisenacher M; Perez E; Uszkoreit J; Pfeuffer J; Sachsenberg T; Yilmaz S; Tiwary S; Cox J; Audain E; Walzer M; Jarnuczak AF; Ternent T; Brazma A; Vizcaino JA Nucleic Acids Res. 2019, 47, D442–D450. [PubMed: 30395289]

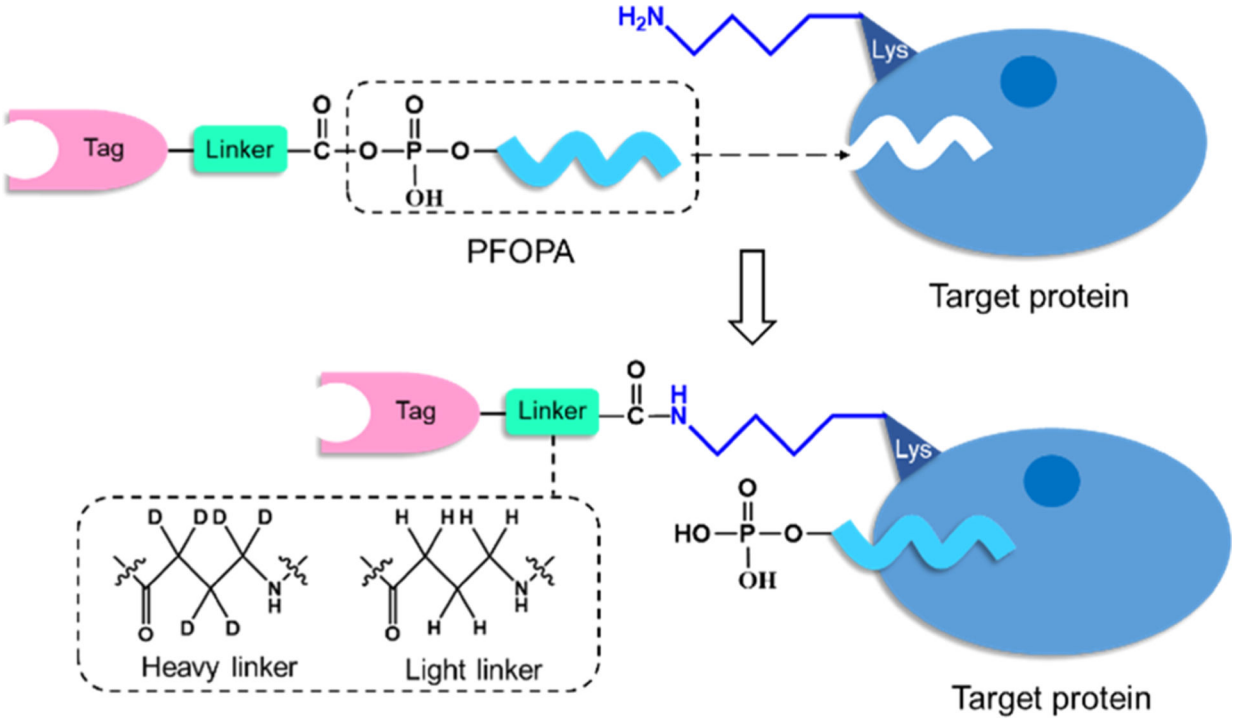

Figure 1.

Design of an isotope-labeled affinity probe for the conjugation and enrichment of PFOPA-binding proteins.

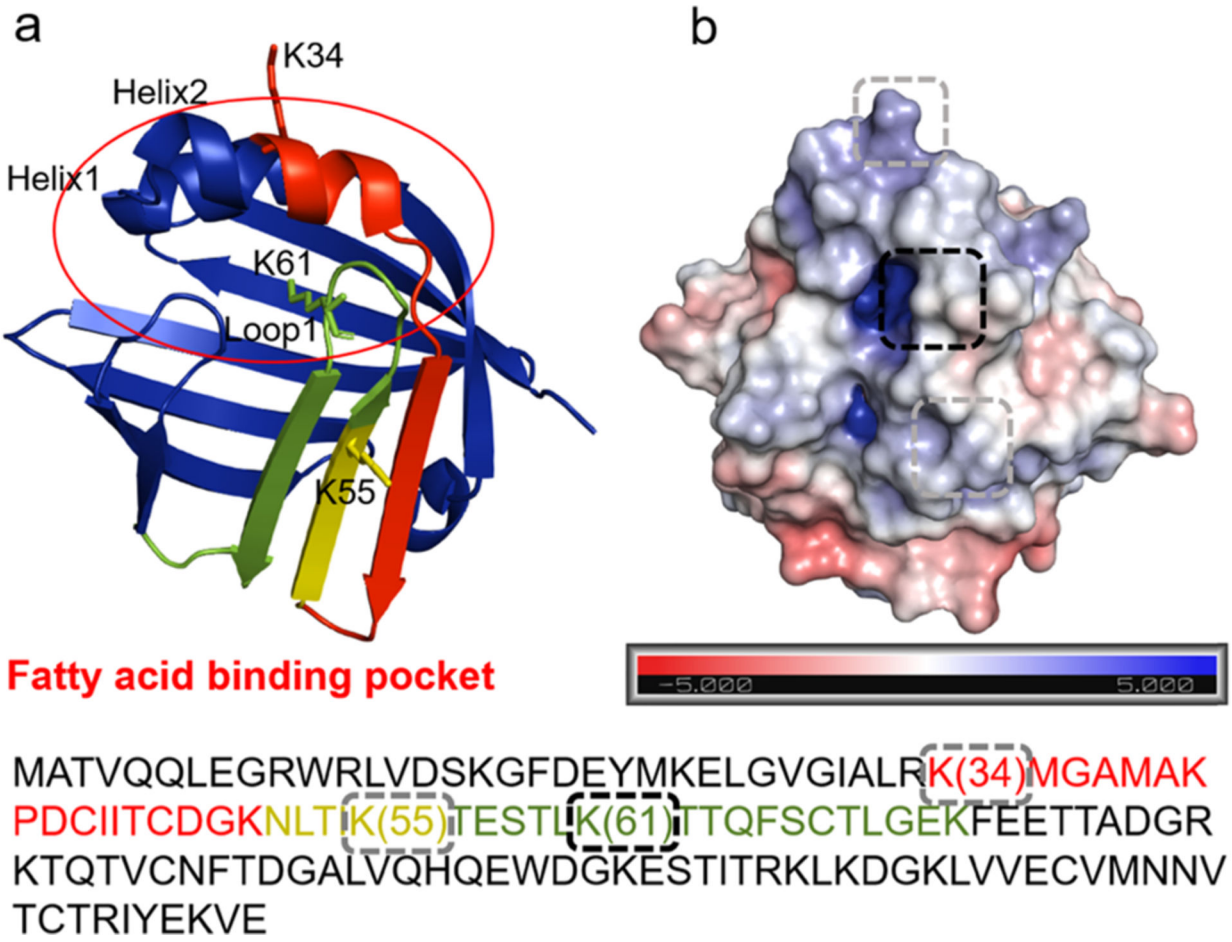

Figure 2.

X-ray crystal structure of FABP5 and desthiobiotin-labeled tryptic peptides identified from shotgun proteomic analysis. The red circle in (a) marks the portal region of FABP5, including loop 1, helix 1, and helix 2. The desthiobiotin-modified lysine is highlighted in stick mode. (b) Surface electrostatic potential map of FABP5. Shown below the structures are the primary amino acid sequence of FABP5, and the amino acids from the three identified desthiobiotin-conjugated peptides are labeled in different colors. The desthiobiotin-modified lysine is highlighted with dashed rectangles.

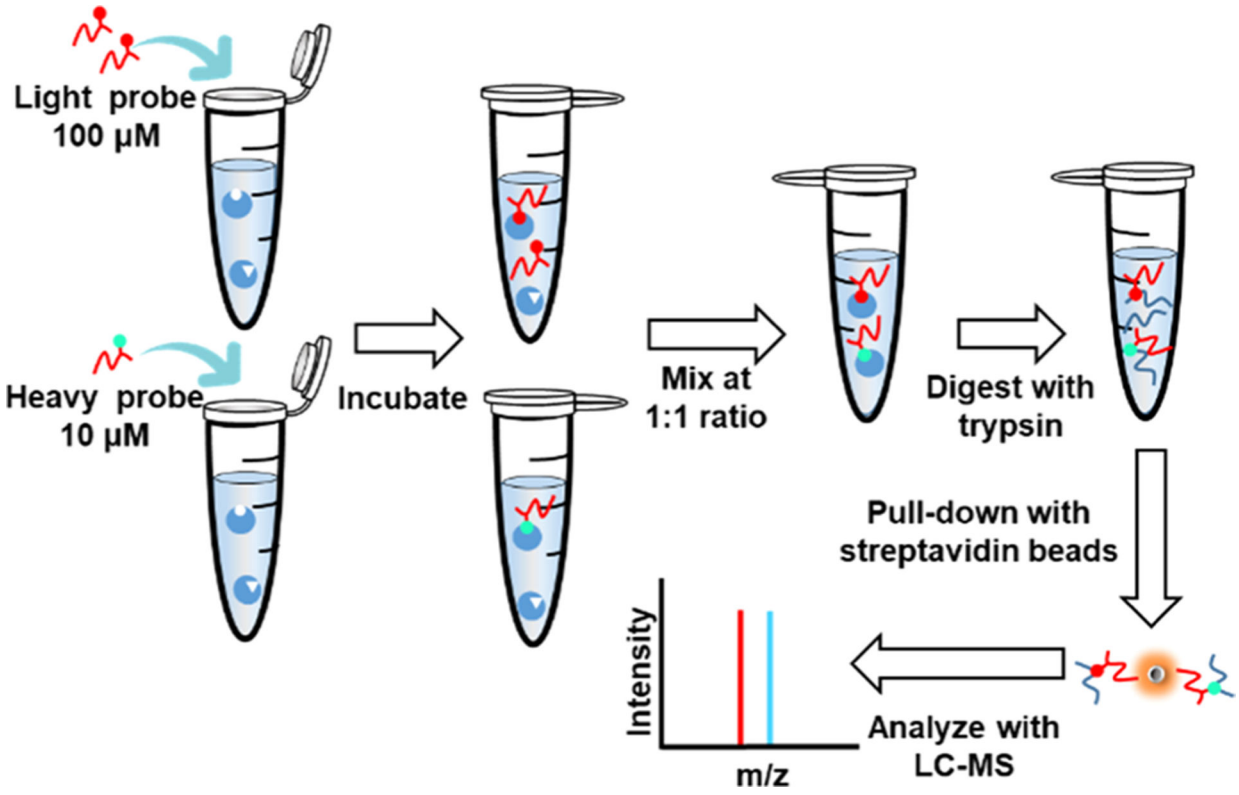

Figure 3.
General workflow for the proteome-wide profiling of PFOPA-binding proteins using stable isotope-labeled desthiobiotin-PFOPA acyl phosphate probes.

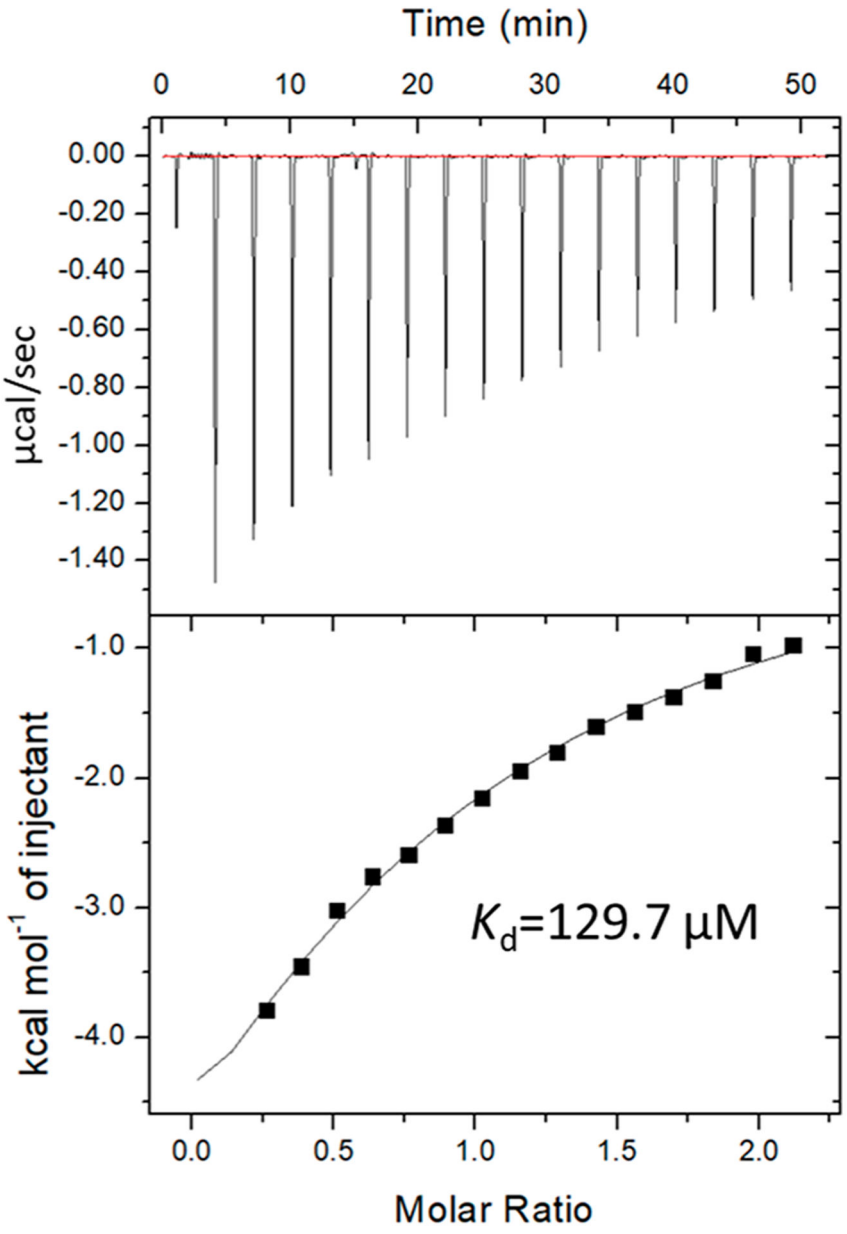

Figure 4.

ITC for determining dissociation constants between FABP5 and PFOPA. FABP5 solution was titrated over 0.1 mM PFOPA in a buffer containing 30 mM Tris–HCl (pH 7.5), 100 mM NaCl, and 5% glycerol at 25 °C.